Extended Abstracts of the 2004 International Conference on Solid State Devices and Materials, Tokyo, 2004, pp. 528-529

Thermal Stability and Electrical Properties of $(La_2O_3)_{1-x}(Al_2O_3)_x$ Composite Films

Ryota Fujitsuka, Mitsuo Sakashita, Akira Sakai, Shigeaki Zaima, and Yukio Yasuda*

Graduate School of Engineering, Nagoya University, Furo-cho, Chikusa-ku, Nagoya 464-8603, Japan
Phone: +81-52-789-3819, Fax: +81-52-789-2760, E-mail: sakasita@alice.xtal.nagoya-u.ac.jp

1. Introduction

La_2O_3 is an attractive candidate for high-*k* materials. However, its thermal stability is one of the key problems including crystallization [1], growth of the low-*k* interfacial layer [2], and diffusion of Si or transformation into silicate [3] during deposition or subsequent thermal annealing. Therefore, controlling these factors is important to attain desirable electrical properties. Adding Al_2O_3 is a promising approach to improve the thermal stability of La_2O_3. Al_2O_3 is known to have superior thermal stability and it has been reported that adding Al_2O_3 to HfO_2 has an effect in raising the crystallization temperature of HfO_2 [4] and suppressing growth of the interfacial SiO_x layer during high temperature annealing [5].

In this work, we have synthesized $(La_2O_3)_{1-x}(Al_2O_3)_x$ composite films (x=0.00, 0.20, 0.33, 0.50) and examined the effects of adding Al_2O_3 to La_2O_3 from a viewpoint of thermal stability and electrical properties.

2. Experiments

Samples were prepared by a pulsed laser deposition (PLD) method with La_2O_3 and Al_2O_3 targets. $(La_2O_3)_{1-x}(Al_2O_3)_x$ composite films were formed by stacking ultra-thin La_2O_3 and Al_2O_3 layers on HF-treated n-Si (100) substrates, as shown in Fig. 1. The composite ratio was controlled by changing thicknesses of individual La_2O_3 and Al_2O_3 layers, and the total thickness was set to be 4 nm for all samples. The substrate temperature and ambient oxygen pressure during deposition were 400°C and 20 Pa, respectively. After the deposition, rapid thermal annealing (RTA) was performed at 1000°C for 15 sec in a N_2 ambient.

Cross-sectional transmission electron microscopy (XTEM) and X-ray photoelectron spectroscopy (XPS) were used to analyze the structural properties. The electrical properties were evaluated by measuring the capacitance-voltage (C-V) and current-voltage (J-V) characteristics using MIS capacitors with Pt top electrodes.

3. Results and Discussion

Figures 2(a) and 2(b) show XTEM images of as-grown $(La_2O_3)_{1-x}(Al_2O_3)_x$ films with the composite ratios of x=0.00 and x=0.50, respectively. An amorphous structure and an interlayer with a thickness of 0.8 and 1.0 nm were observed for the x=0.00 and the x=0.50 samples, respectively. Figure 3 shows XTEM images of RTA-treated samples with the same composite ratios as those shown in Fig. 2. The x=0.00 sample (Fig. 3(a)) was uniformly crystallized and polycrystalline grains with lattice fringes were observed. These grains should come from La-silicate phases since the observed lattice spacing of 0.29 nm does not correspond to that of La_2O_3, and La 3d and O 1s XPS spectra showed the existence of La-silicate in the film (not shown). On the other hand, the x=0.50 sample (Fig. 3(b)) remained the amorphous structure. These results clearly indicate that adding Al_2O_3 is effective in suppressing crystallization after RTA. This effect was also confirmed in the x=0.33 sample. Furthermore, it was clearly observed in all RTA-treated samples that the interlayer formed during deposition became thinner. This should be due to the intermixing of the interlayer with the upper $(La_2O_3)_{1-x}(Al_2O_3)_x$ layer to form a La-aluminate-silicate phase.

Changes of Si 2s core-level XPS spectra before and after RTA are shown in Fig. 4. For all samples, the Si sub-oxide peak intensity increased after RTA, but the increase is more suppressed for the higher Al_2O_3 composition samples. Considering the XTEM results that the interlayer did not grow after RTA, the increase in Si sub-oxide peak intensity is probably attributed to the diffusion of Si into the upper $(La_2O_3)_{1-x}(Al_2O_3)_x$ layer. Therefore, Al_2O_3 addition has an effect in suppressing Si in-diffusion and this effect is closely related to the Al_2O_3 composite ratio.

Figure 5 shows the correlation between the Al_2O_3 composite ratio and the electrical properties for as-grown and RTA-treated samples. The capacitance equivalent oxide thickness (CET) decreased while the leakage current density was degraded after RTA, resulting mainly from the reduction of the interlayer thickness. The smaller CET was obtained for the lower Al_2O_3 composition sample, and the lower leakage current density was obtained for both as-grown and RTA-treated samples with x=0.20 and x=0.33. This leads to an optimum x value of $(La_2O_3)_{1-x}(Al_2O_3)_x$ of 0.20 in the present experiment from a viewpoint of the electrical properties. For this ratio, the CET of 1.2 nm with the leakage current density of 3.9×10^{-3} A/cm^2 (@V_{fb}+1 V) was attained after RTA.

4. Conclusions

We have synthesized $(La_2O_3)_{1-x}(Al_2O_3)_x$ composite films and examined the effects of adding Al_2O_3 to La_2O_3 in terms of thermal stability and electrical properties. Al_2O_3 addition had an effect in suppressing crystallization and the samples with an x value of 0.33 and more could remain the amorphous structure even after RTA at 1000°C for 15 sec. Si diffusion into the film was also suppressed by adding Al_2O_3 and this effect was pronounced for the samples with higher Al_2O_3 ratios.

*present address : Kochi University of Technology, 185 Miyanokuchi, Tosayamada-cho, Kami-gun, Kochi 782-8502, Japan

For all RTA-treated samples, the interlayer formed during deposition became thinner due to the intermixing with the $(La_2O_3)_{1-x}(Al_2O_3)_x$ layer. This increases the effective dielectric constants but degrades the leakage property, which determines optimum composite ratios of the $(La_2O_3)_{1-x}(Al_2O_3)_x$ films.

References

[1] X. Wu, D. Landheer, G. I. Sproule, T. Quance, M. J. Graham, and G. A. Botton: J. Vac. Sci. Technol. **A20**, (2002) 1141.

[2] J. H. Jun, D. J. Choi, K. H. Kim, K. Y. Oh, and C. J. Hwang: Jpn. J. Appl. Phys. **42**, (2003) 3519.

[3] H. Yamada, T. Shimizu, and E. Suzuki: Jpn. J. Appl. Phys. **41**, (2002) 368.

[4] P. F. Lee, J. Y. Dai, K. H. Wong, H. L. W. Chan, and C. L. Choy: J. Appl. Phys. **93**, (2003) 3665.

[5] H. Y. Yu, N. Wu, M. F. Li, Chunxiang Zhu, B. J. Cho, D. -L. Kwong, C .H. Tung, J. S. Pan, J. W. Chai, W. D. Wang, D. Z. Chi, C. H. Ang, J. Z. Zheng, and S. Ramanathan: Appl. Phys. Lett. **81**, (2002) 3618.

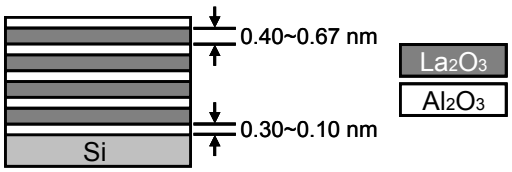

Fig. 1. Schematic diagram of the stacked structure to form the $(La_2O_3)_{1-x}(Al_2O_3)_x$ composite films.

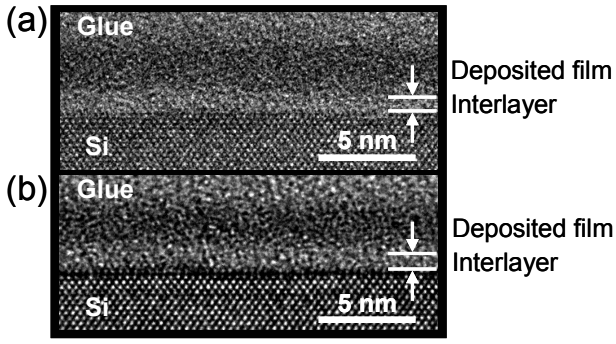

Fig. 2. Cross-sectional TEM images of as-grown $(La_2O_3)_{1-x}(Al_2O_3)_x$ composite films of (a) x=0.00 and (b) x=0.50.

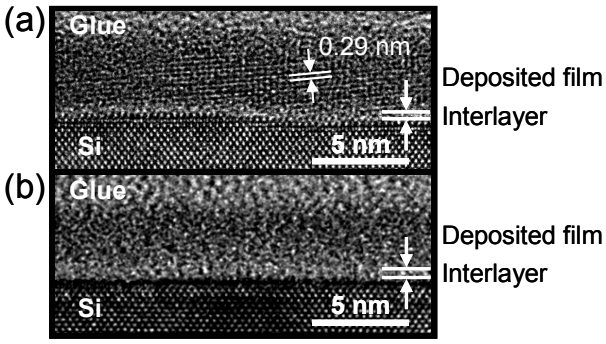

Fig. 3. Cross-sectional TEM images of RTA-treated $(La_2O_3)_{1-x}(Al_2O_3)_x$ composite films of (a) x=0.00 and (b) x=0.50.

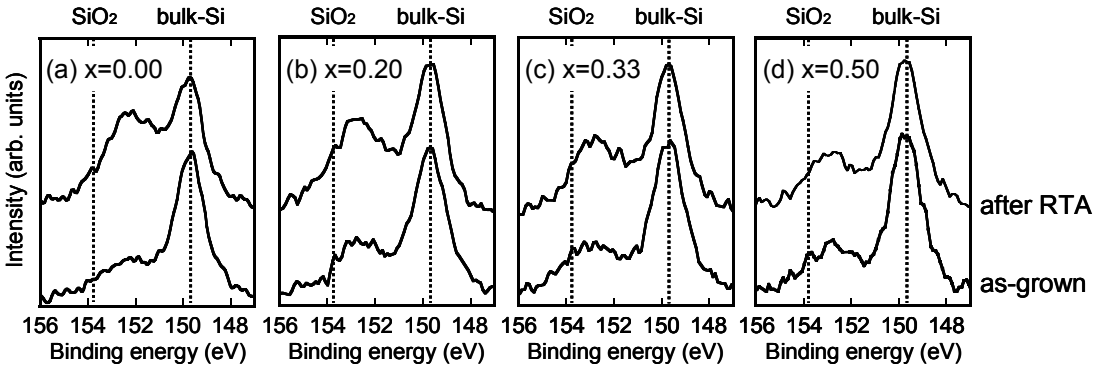

Fig. 4. Si 2s core-level XPS spectra for as-grown and RTA-treated samples with the composition ratios of (a) x=0.00, (b) x=0.20, (c) x=0.33 and (d) x=0.50.

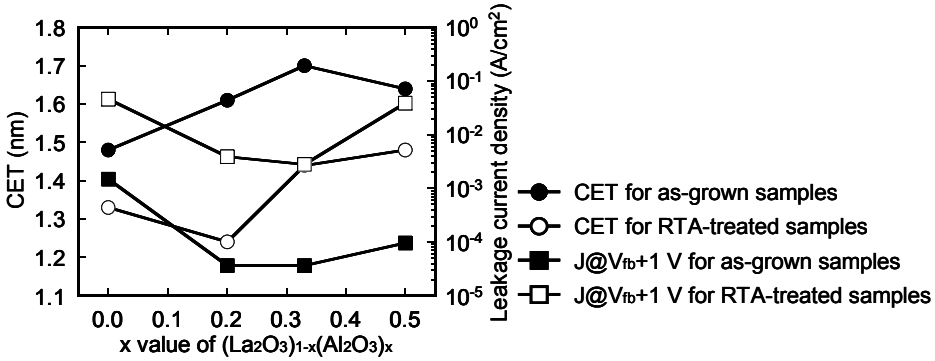

Fig. 5. Relationship between the x value of $(La_2O_3)_{1-x}(Al_2O_3)_x$ and the electrical properties of CET and leakage current density at V_{fb}+1 V.